Autophagy 8:9, 1333-1341; September 2012; © 2012 Landes Bioscience

ATG7 deficiency suppresses apoptosis and cell death induced by lysosomal photodamage

David H. Kessel,[1,*] Michael Price[2] and John J. Reiners, Jr.[3]

[1]Department of Pharmacology, Wayne State University School of Medicine, Detroit, MI USA; [2]Cancer Biology Program, Wayne State University, Detroit, MI USA; [3]Institute of Environmental Health Sciences, Wayne State University, Detroit, MI USA

Keywords: apoptosis, autophagy, subcellular localization, lysosomes, photodynamic therapy

Abbreviations: ATG7, autophagy-related protein 7; KD, ATG5 or ATG7 knockdown 1c1c7 cells; ER, endoplasmic reticulum; LD_{xx}, lethal dose–the subscript indicates the percent loss of viability; LTR, LysoTracker Red; NPe6, mono-L-aspartyl chlorin e6; Pc 4, a phthalocyanine-based photosensitizing agent; PDT, photodynamic therapy; ROS, reactive oxygen species; WT, wild-type 1c1c7 cells; WST9, a palladium bacteriopheophorbide; WST11, a water-soluble palladium bacteriopheophorbide

Photodynamic therapy (PDT) involves photosensitizing agents that, in the presence of oxygen and light, initiate formation of cytotoxic reactive oxygen species (ROS). PDT commonly induces both apoptosis and autophagy. Previous studies with murine hepatoma 1c1c7 cells indicated that loss of autophagy-related protein 7 (ATG7) inhibited autophagy and enhanced the cytotoxicity of photosensitizers that mediate photodamage to mitochondria or the endoplasmic reticulum. In this study, we examined two photosensitizing agents that target lysosomes: the chlorin NPe6 and the palladium bacteriopheophorbide WST11. Irradiation of wild-type 1c1c7 cultures loaded with either photosensitizer induced apoptosis and autophagy, with a blockage of autophagic flux. An ATG7- or ATG5-deficiency suppressed the induction of autophagy in PDT protocols using either photosensitizer. Whereas ATG5-deficient cells were quantitatively similar to wild-type cultures in their response to NPe6 and WST11 PDT, an ATG7-deficiency suppressed the apoptotic response (as monitored by analyses of chromatin condensation and procaspase-3/7 activation) and increased the LD_{50} light dose by > 5-fold (as monitored by colony-forming assays). An ATG7-deficiency did not prevent immediate lysosomal photodamage, as indicated by loss of the lysosomal pH gradient. However, unlike wild-type and ATG5-deficient cells, the lysosomes of ATG7-deficient cells recovered this gradient within 4 h of irradiation, and never underwent permeabilization (monitored as release of endocytosed 10-kDa dextran polymers). We propose that the efficacy of lysosomal photosensitizers is in part due to both promotion of autophagic stress and suppression of autophagic prosurvival functions. In addition, an effect of ATG7 unrelated to autophagy appears to modulate lysosomal photodamage.

Introduction

Photodynamic therapy (PDT) is a process wherein irradiation of a photosensitizing agent leads to the conversion of molecular oxygen in cells and tissues to a series of reactive oxygen species (ROS), with cytotoxic consequences. This can result in selective photodamage to malignant tissues and their vasculature.[1,2] Oleinick's group was the first to demonstrate that PDT can trigger an apoptotic death program.[3] This has been related to destructive effects of PDT-generated ROS on the anti-apoptotic proteins BCL2 and BCL2L1/Bcl-X_L.[4-6] Oxidative inactivation of BCL2 can also elicit an autophagic response, e.g., via release of BECN1 from a BCL2 complex.[7]

Many photosensitizers accumulate preferentially in specific organelles (e.g., late endosomes/lysosomes, mitochondria, or the endoplasmic reticulum).[8-10] In such cases, subsequent irradiation causes very specific organelle photodamage. Although the initial targets for photodamage can vary with the choice of photosensitizer, the induction of autophagy commonly occurs in PDT protocols, irrespective of the photosensitizing agent.[10] In the context of PDT, the induction of macroautophagy (referred to here as 'autophagy') often functions as a survival response in cells capable of developing an apoptotic response.[10-12] However, if pathways to apoptosis are impaired, autophagy may play a role in cell death.[10,13]

We recently reported that shRNA knockdown of *Atg7* suppressed the development of autophagy, and reduced the light-dose needed to kill murine hepatoma 1c1c7 cells loaded with either mitochondrial or endoplasmic reticulum (ER) photosensitizers.[10,11] These results are consistent with the proposal that autophagy plays a prosurvival role under these conditions. After lysosomal photodamage, we have shown that autophagosomes

*Correspondence to: David H. Kessel; Email: dhkessel@med.wayne.edu
Submitted: 10/25/11; Revised: 05/15/12; Accepted: 05/17/12
http://dx.doi.org/10.4161/auto.20792

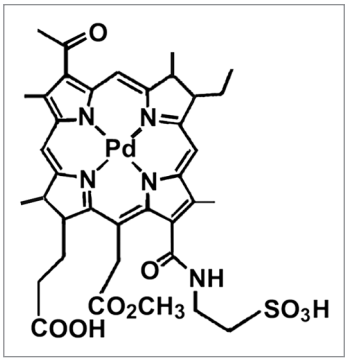

Figure 1. Structure of WST11.

are formed.[10] It seems likely that subsequent steps in the autophagic pathway would be blocked because of the lack of functional lysosomes. Such a blockage might suppress the potential prosurvival effects of autophagy and/or actually contribute to the cytotoxicity of the photosensitizer. This study was designed to assess these possibilities and involves comparisons between wild-type cultures and cell lines deficient in either ATG7 or ATG5. Two lysosomal photosensitizers were employed, the chlorin NPe6 (N-aspartyl chlorin e6, Taliporfin)[14,15] and the palladium bacteriopheophorbide designated WST11 (**Fig. 1**).[16,17] Although the lysosomal accumulation of NPe6 is well characterized,[18-20] we were initially uncertain about the pattern of WST11 cellular localization. Once we established that WST11 localized to lysosomes, it was included in this study. Our studies demonstrate that autophagic flux is suppressed in cells with photodamaged lysosomes, and that ATG7, but not ATG5, is required for the development of an apoptotic response in such cells. As such, ATG7 appears to differentially modulate the cytotoxicities of photosensitizers that target lysosomes vs. mitochondria or the ER.

Results

Subcellular localization of photosensitizers. The preferential accumulation of NPe6 in lysosomes has been independently established by several groups.[18-20] Although Mazor et al. postulated an endocytic mechanism for WST11 accumulation,[16] very little is known about the subcellular localization of WST11. We could detect intracellular WST11 fluorescence only with an electron-multiplying CCD camera. WST11 exhibited distinct fluorescent puncta in both wild-type and ATG7 KD 1c1c7 cell types (**Fig. 2A and B**). Because of its very low fluorescence yield, it was not feasible to monitor colocalization of WST11 with commonly employed fluorescent probes for endosomes and lysosomes, since their fluorescence emission spectra tail into the far red. As an alternative approach, we assessed the effects of WST11 PDT on the fluorescence of LysoTracker Red (LTR). This probe accumulates in acidic organelles to yield bright red fluorescent puncta. Procedures that disrupt such organelles will cause the loss of this fluorescent pattern.[19,20] Both wild-type and ATG7 KD 1c1c7 cultures exhibited well defined, strong LTR fluorescent puncta (**Fig. 2C and D**, respectively). Irradiation of either cell type

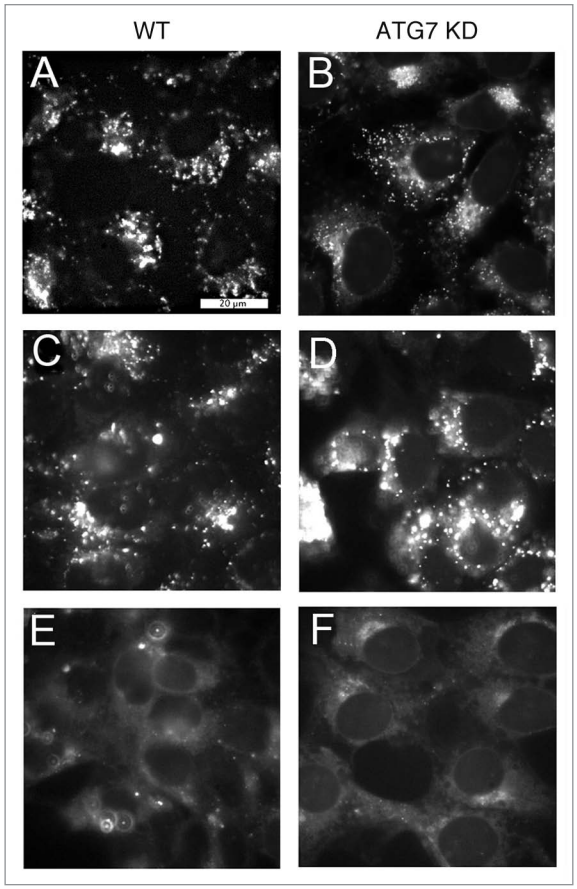

Figure 2. Subcellular localization of WST11 and effects on LTR fluorescence. Fluorescence localization patterns of WST11 in WT (A) or ATG7 KD (B) cultures after a 16 h incubation with 1 μM drug. (C–F) Effects of photodamage on the pattern of LTR fluorescence. Wild-type (C and E) or ATG7 KD cultures (D and F) were photosensitized with 1 μM WST11 for 16 h, then treated with LTR for 10 min before (C and D) or directly after (E and F) irradiation (90 mJ/cm^2). White bar in (A): 20 μm. Photographs are representative of observations for three independent experiments.

previously photosensitized with WST11 (1 μM, 16 h) resulted in the loss of punctate LTR fluorescence, consistent with lysosomal/endosomal photodamage (**Fig. 2E and F**). Analyses similar to those presented in **Figure 2** with WT cells were also performed with fluorescent probes that label mitochondria (MitoTracker Orange) and the endoplasmic reticulum (ER-Tracker). Irradiation of WST11-loaded WT cultures had no effects on the fluorescence distribution or intensity of either probe (**Fig. S1**).

Phototoxicity. A light-response survival study was performed using wild-type and ATG7 KD 1c1c7 cells photosensitized by a 16 h exposure to 1 μM WST11. Colony formation assays revealed that the ATG7 KD line, relative to wild-type cultures, was markedly resistant to phototoxicity (**Fig. 3**). Even at a light dose of 405 mJ/cm^2, sufficient for a ~2 log kill of WT cells, the corresponding loss of viability in the ATG7 KD line was only 30%. In order to determine whether this difference was related to differential capacities for developing an autophagic response, we also examined the effects of WST11 on ATG5 KD 1c1c7 cultures (**Fig. S2**

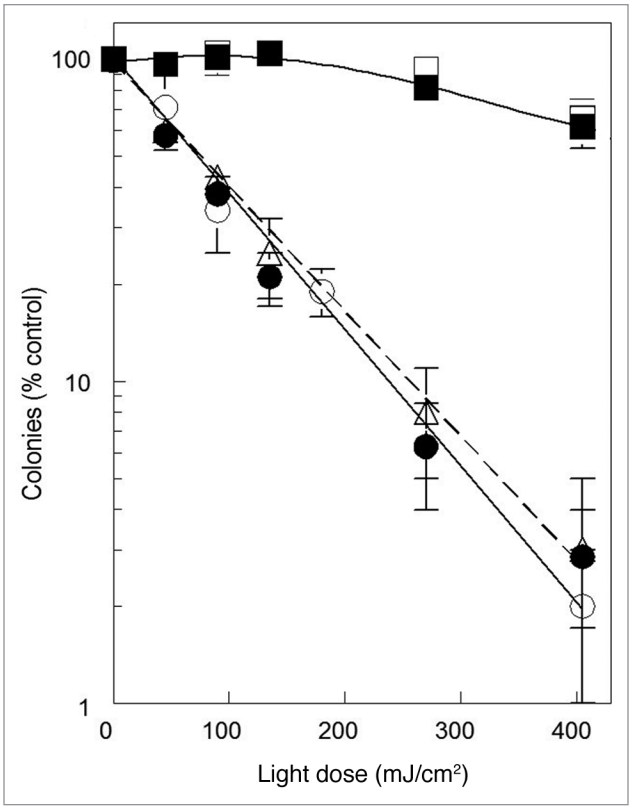

Figure 3. Effects of WST11 and NPe6 on 1c1c7 survival. Cultures of wild type (●, ○), ATG7 KD (■, □), and ATG5 KD (△) 1c1c7 cells were sensitized with 1 μM WST11 for 16 h (●, ■, △) or 20 μM NPe6 for 1 h (○, □) prior to being irradiated for different lengths of time to achieve the indicated light doses. Results with ATG5 KD cells are indicated by a dashed line. Colonies of 30 or more cells were determined 5 d later. Data are normalized to no-treatment controls and represent mean ± SD of three determinations. Similar results were obtained in a second independent experiment.

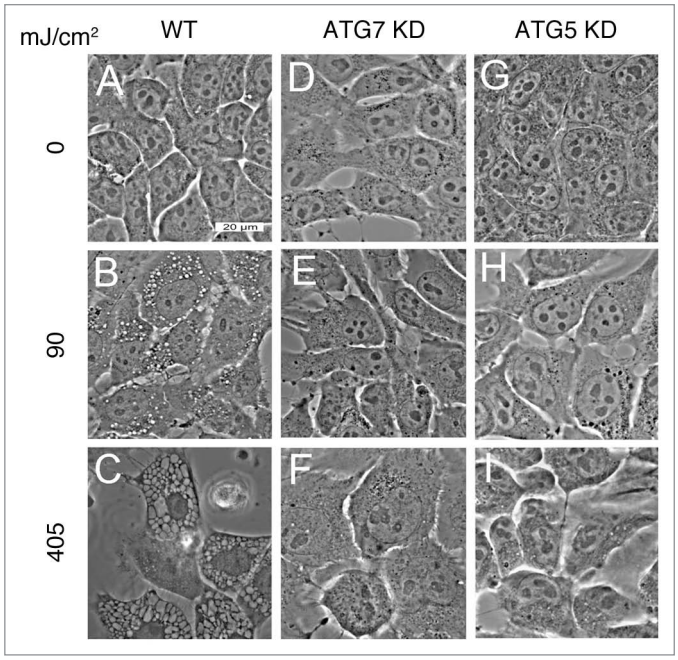

Figure 4. WST11 induced vacuolization. Cultures of wild-type (A–C), ATG7 KD (D–F) and ATG5 KD (G–I) 1c1c7 cells were incubated with 1 μM WST11 for 16 h prior to irradiation with light doses of 0 (A–G), 90 mJ/cm² (B,E and H), or 405 mJ/cm² (C, F and I). Images were captured 2 h after irradiation. Bar in (A): 20 μm. Images are representative of three independent experiments.

documents ATG5 knockdown). In contrast to what was observed with the ATG7 KD cells, the ATG5 KD line was as responsive as WT cells to photodamage (**Fig. 3**, dashed line).

NPe6 also accumulates in the lysosomes/endosomes of wild-type 1c1c7 cells, and induces both apoptosis and autophagy following irradiation.[10,19-21] A comparison of the response of wild-type and ATG7 KD cells to NPe6 PDT was performed after a 1 h loading with sensitizer (**Fig. 3**). The NPe6 concentration and loading conditions were chosen to closely approximate the dose-response curve obtained with WST11 in WT cells, and were based upon previously published survival curves.[21] Dose-response survival curves for the ATG7 KD line after NPe6 or WST11 PDT were essentially identical (**Fig. 3**). Hence, the absence of ATG7 similarly suppressed the toxicity of two different photosensitizers that preferentially accumulate in acidic vesicles.

Effects of PDT on cellular morphology and induction of autophagy. Exposure of wild-type 1c1c7 cells, photosensitized with WST11, to an LD_{60} or an LD_{95} PDT light dose led to the light dose-dependent formation of cytoplasmic vacuoles (**Fig. 4A–C**). These vacuoles were readily detectable within 2 h of irradiation and were larger and more numerous in cells treated with the higher light dose (compare **Fig. 4B and C**). Similar PDT conditions did not induce vacuole formation in ATG7 KD cells, although some cellular swelling was observed after the higher light dose (**Fig. 4D–F**). WST11 photosensitized ATG5 KD cultures also lacked cytoplasmic vacuoles following irradiation (**Fig. 4G–I**).

Previous studies suggested that PDT-induced vacuolization is often accompanied by the induction of autophagy.[10] Wild-type cells that stably express a GFP-LC3 fusion protein exhibited diffuse fluorescence (**Fig. 5A and B**). GFP coalesced into fluorescent puncta within 1 h of irradiation of WST11 sensitized cultures with a LD_{95} light dose (**Fig. 5C and D**), and persisted for at least an additional 3 h (**Fig. 5E and F**). Presumably these GFP-LC3 fluorescent puncta represent autophagosomes. Vesicles exhibiting a double-walled membrane, which are characteristic of autophagosomes,[22] were apparent within 4 h of irradiation (**Fig. 5G**). Moreover, western blot analyses of wild-type cultures documented the conversion of LC3-I into LC3-II within 2 h of irradiation (**Fig. 5H**, lanes 1 vs. 3), another indicator of autophagy.[22] The lysosomotropic agent NH_4Cl raises lysosomal pH, reduces the activities of lysosomal proteases, and suppresses autophagic flux.[22] Treatment of cultures with NH_4Cl had no effect on LC3-II content after PDT (**Fig. 5H**, lanes 3 vs. 4). This is consistent with the processing of autophagosomes being blocked by WST11-induced photodamage to lysosomes. Relative to wild-type cultures, ATG7 KD cells exhibited reduced levels of LC3-II in both nontreated cultures (**Fig. 5H**, lanes 1 vs. 2) and following irradiation (**Fig. 5H**, lane 3 vs. 5). The addition of NH_4Cl had

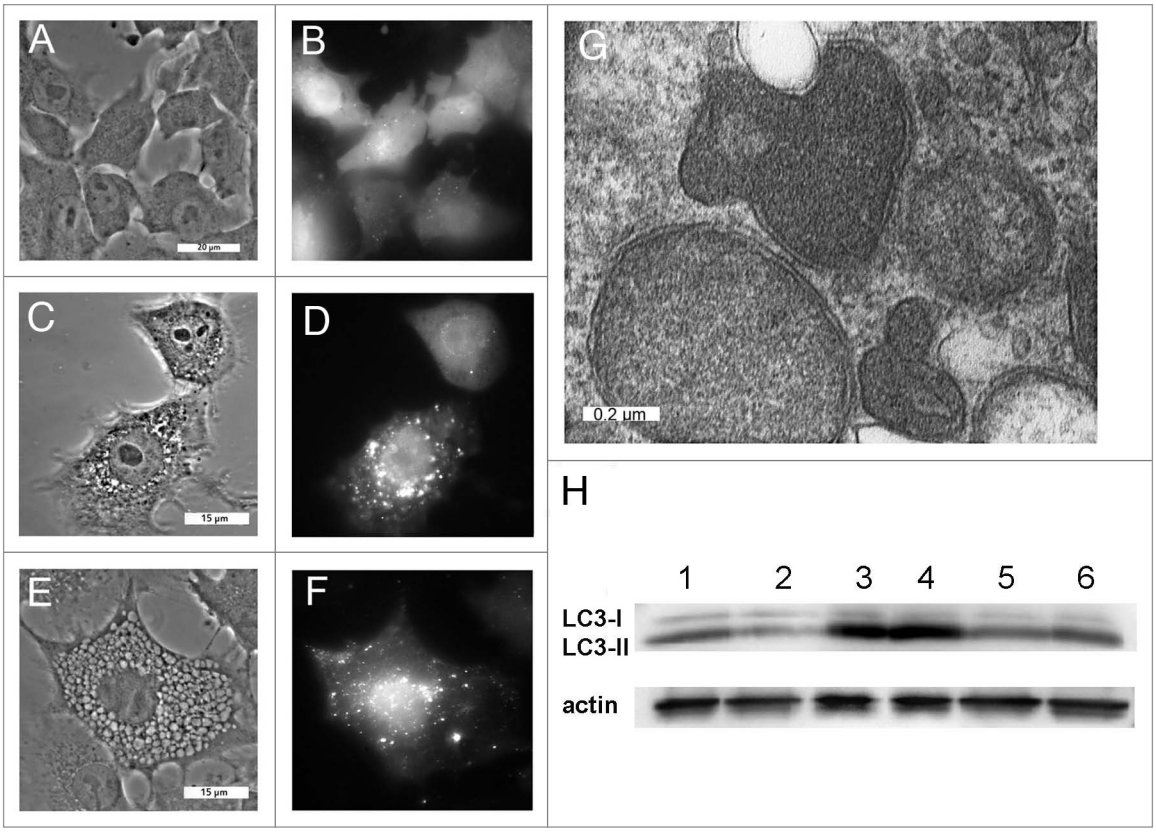

Figure 5. WST11 induction of autophagy. Cultures of GFP-LC3-expressing wild-type 1c1c7 cells were incubated with 1 μM WST11 for 16 h prior to being imaged by phase and fluorescence microscopy immediately prior to (A and B), 1 h (C and D) or 4 h (E and F) after irradiation (405 mJ/cm^2). White bars: (A and B) 20 μm; (C–F) 15 μm. (G) Electron micrograph of representative autophagosomes found in WT 1c1c7 cultures loaded with 1 μM WST11 for 16 h and fixed for processing 4 h after irradiation with 405 mJ/cm^2. White bar: 0.2 μm. (H) Western blot analysis of LC3 and actin in untreated WT (lane 1) or ATG7 KD (lane 2) cells. Alternatively, WT (lanes 3 and 4) and ATG7 KD cells (lanes 5 and 6) were incubated for 16 h with WST11 prior to exposure to a 405-J/cm^2 light dose. NH_4Cl (50 mM) was added to some cultures immediately after irradiation (lanes 4 and 6). All cultures were harvested 2 h after irradiation. Similar results were obtained in a second independent study.

little effect on the accumulation of LC3-II in irradiated ATG7 KD cultures (**Fig. 5H**, lanes 5 vs. 6).

PDT-induced apoptosis. In addition to intense vacuolization, we also noted that wild-type cells exhibited apoptotic features after WST11-induced photodamage and were released from the culture dishes. Chromatin condensation is a characteristic of apoptotic cells and can be monitored by labeling of nuclei with HO33342.[21,23] Attached cells with condensed chromatin were not detected in untreated WT cultures (**Fig. 6A**, a) or 1 h after treatment with LD_{60} or LD_{95} doses (**Fig. 6A**, b and c), or 4 h after treatment with an LD_{60} light dose (**Fig. 6A**, d). However, attached cells with condensed chromatin were detected in cultures 4 h after treatment with a LD_{95} light dose (arrows, **Fig. 6A**, e). Within 24 h of irradiation almost every cell in the LD_{95} treatment group had detached and exhibited condensed chromatin (**Fig. 6A**, g). In contrast, a significant number of cells remained attached in the LD_{60} treatment group and exhibited a normal chromatin staining pattern (left half of **Fig. 6A**, f). Cells that had detached exhibited condensed chromatin (right half of **Fig. 6A**, f). In contrast to WT cells, ATG7 KD cells neither detached from the culture dishes nor exhibited condensed chromatin following sensitization with WST11 and irradiation with the same light doses (**Fig. 6A**, h–n). ATG5 KD cells behaved like WT cells in their response to WST11 PDT (**Fig. S3**). Adherent cells with condensed chromatin were observed within 4 h of irradiation with a LD_{90} light dose (**Fig. S3C**). Within 24 h of irradiation virtually every cell had detached from the culture dishes and exhibited condensed chromatin (**Fig. S3D**).

DEVDase activity is commonly used to monitor the conversion of procaspases-3 and -7 into their active forms. This approach has been used to monitor the development of apoptosis after photodamage.[19-21] Exposure of WST11- or NPe6-sensitized wild-type 1c1c7 cultures to LD_{60} or LD_{95} light doses elevated DEVDase activities above background activities, in a dose-dependent fashion, within 4 h of irradiation (**Fig. 6B**). During the same time course, following similar treatment with the highest light dose, only a slight activation of DEVDase occurred in ATG7 KD cultures (**Fig. 6B**). In contrast, both the kinetics and magnitude of DEVDase activation in ATG5 KD cells was comparable to that measured in WT cells.

PDT-induced lysosome permeabilization. Irradiation of WST11-photosensitized WT or ATG7 KD cultures with a 90-mJ/cm^2 light dose caused a substantial loss of the LTR labeling

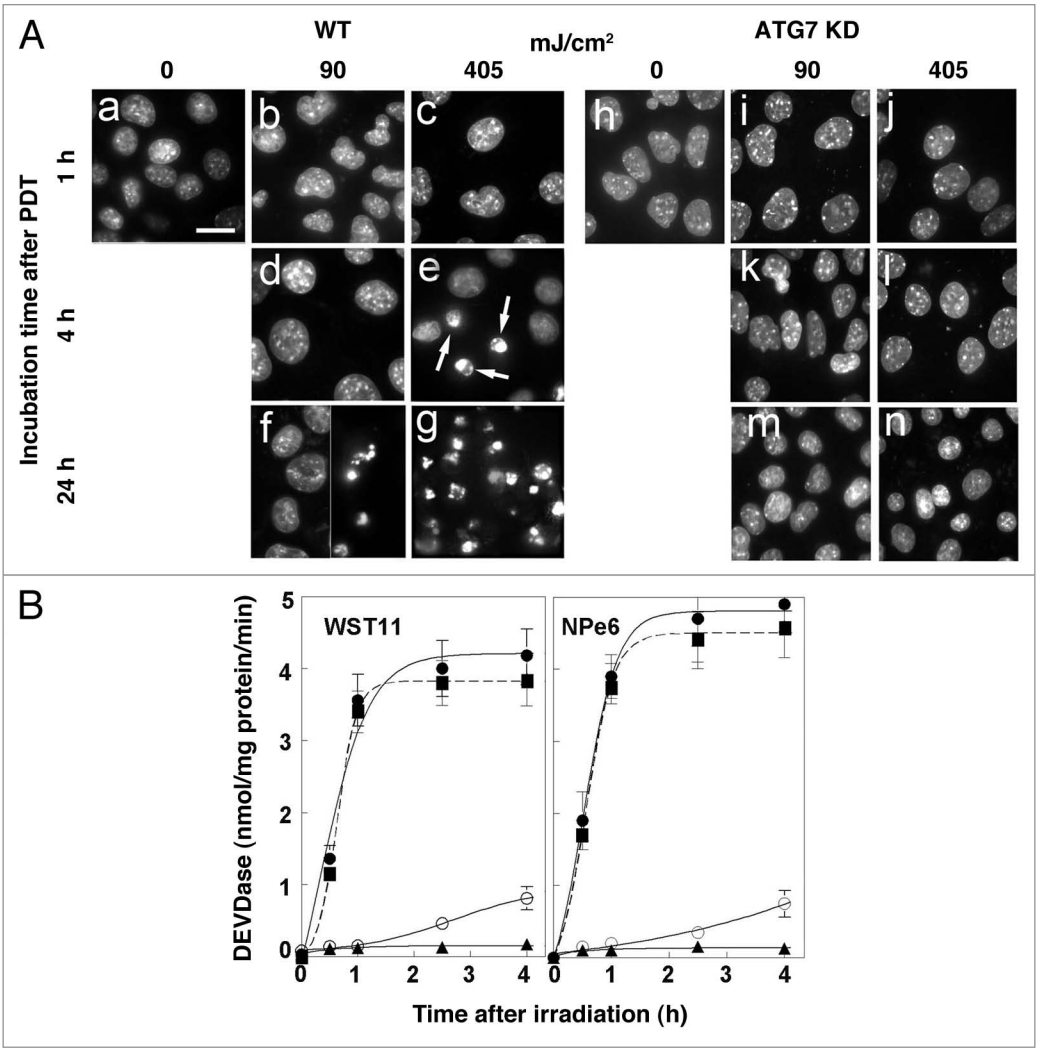

Figure 6. Effects of WST11 PDT on nuclear morphology and procaspase activation. (A) Cultures of wild-type (a–g) and ATG7 KD (h–n) 1c1c7 cells were loaded with 1 μM WST11 for 16 h prior to no treatment, or irradiation (90 or 405 mJ/cm²). Cultures were subsequently incubated with HO33342 for 10 min prior to being imaged 1, 4 or 24 h after irradiation. With the exceptions of (g) and the right half of (f), all other images are of adherent cells. (g) and the right half of (f) are images of HO33342 stained non-adherent floating cells which constitute ~50% and > 95% of all the cells in the plates, respectively. Arrows in (e) point to nuclei with condensed chromatin. Bar in (a): 20 μm. (B) Cultures of wild-type (●, ○), ATG7 KD (▲) or ATG5 KD (■) 1c1c7 cells were treated with 1 μM WST11 for 16 h or with 20 μM NPe6 for 1 h prior to irradiation with either 90 mJ/cm² (○) or 405 mJ/cm² (●, ▲, ■). Cultures were harvested at specified times after irradiation for analyses of DEVDase activity. Data represent means ± SD of three analyses at each time point for all treatment groups. Similar results were obtained in a second independent study.

pattern in both cell lines (**Fig. 2**). This light dose caused a 60% loss of viability for WT cells, but had no effect on ATG7 KD cell survival (**Fig. 3**). In order for the ATG7 KD cells to survive, they must recover rapidly from lysosomal photodamage. To test this assumption, we examined the effects of a 405-mJ/cm² light dose on cells photosensitized with WST11 (**Fig. 7**). Results obtained with the ATG7 KD cell line are shown in **Figure 7, a–d**. The initial loss of punctate LTR fluorescence following irradiation (**Fig. 7**, compare a and b) was partly reversed within 4 h (**Fig. 7, c**) and completely reversed after 16 h (**Fig. 7, d**). In a similar study with WT cultures (**Fig. 7, e–h**), no recovery of punctate LTR staining was observed following irradiation. The few adhering cells that remained 16 h after irradiation showed a highly vacuolated morphology with no distinct pattern of LTR fluorescence (**Fig. 7, h**). The loss of punctate LTR fluorescence was also irreversible in irradiated ATG5 KD cells (**Fig. 7, i–l**). Floating cells and cell fragments had no distinct pattern of LTR fluorescence (**Fig. 7, l**).

Loss of punctate LTR fluorescence following WST11 or NPe6 PDT could reflect either inactivation of lysosome-associated proton pumps, or frank permeabilization of the lysosomal membrane. Wild-type 1c1c7 cultures take up fluorescein-conjugated 10 kDa dextran polymers by endocytosis, and accumulate such molecules in lysosomes.[20] Both WT and ATG7 KD cells exhibited bright fluorescent dextran puncta following a 6 h loading period and a 16 h chase period (**Fig. 8D and J**). NPe6 PDT (LD_{95} conditions) caused the loss of both LTR and fluorescent dextran puncta in WT cultures. The loss of LTR puncta preceded the

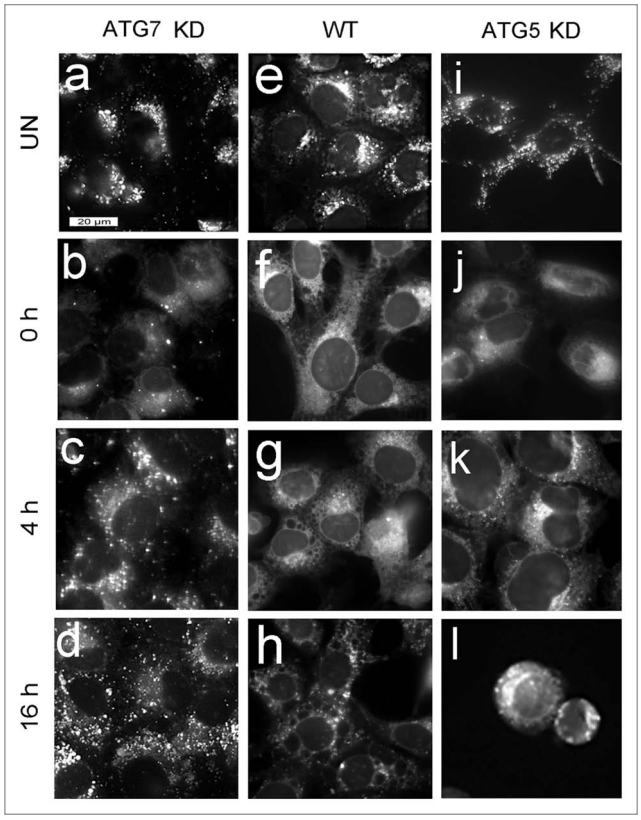

Figure 7. Effects of WST11 PDT on LTR labeling. WT, ATG5 KD and ATG7 KD cultures were left untreated (a, e and i) or incubated with 1 μM WST11 for 16 h prior to being irradiated (405 mJ/cm^2), and labeled with LTR immediately (b ,f and j), 4 h (c, g and k) or 16 h (d, h and l) after irradiation. Bar in (a): 20 μm.

loss of dextran puncta (compare **Fig. 8A–C** with **Fig. 8D–F**). Fluorescent dextran puncta were clearly visible within 10 min of PDT, whereas LTR puncta were absent. However, within 4 h of PDT fluorescent dextran puncta were dramatically reduced in WT cells (**Fig. 8F**), suggesting that the lysosomal membranes had been rendered permeable to large molecules. In contrast, a similar PDT dose caused only a transitory loss of LTR puncta in ATG7 KD cells that was reversed within 4 h of PDT (**Fig. 8I and J**). Unlike what was observed in WT cultures, there was no significant effect on fluorescent dextran puncta in ATG7 KD cultures over the same time period (**Fig. 8J–L**).

Discussion

The palladium bacteriopheophorbide WST11 is a useful photosensitizer because it is activated by the longer wavelengths of light that favor tissue penetration. It is currently being evaluated for treatment of prostate cancer.[17] Fluorescence imaging was consistent with a lysosomal localization pattern for WST11. This could not be confirmed by colocalization studies involving organelle-specific fluorescent probes because of a very low fluorescence yield. Irradiation of cultures photosensitized by either WST11 or NPe6 resulted in loss of the punctate fluorescence that is characteristic of LTR accumulation in late endosomes/lysosomes (**Fig. 2**). This would be expected if photodamage disrupted the pH gradient across the lysosomal membrane, or actually permeabilized the organelles. Our finding that irradiation of WST11-sensitized cultures did not modify the patterns or intensities of fluorescent mitochondrial or ER probes further argues for the lysosomal specificity of WST11 (**Fig. S1**).

Irradiation of WST11 in aqueous solution or bound to serum albumin results in the formation of radical species ($^{\bullet}OH$ and $^{\bullet}O_2^-$) but not singlet oxygen.[24] We recently confirmed that WST11 does not generate singlet oxygen in cultured 1c1c7 cells following photoactivation.[25] This represents a significant departure from the situation with other sensitizers, such as NPe6, where PDT initially generates a high quantum yield of singlet oxygen.[15,26,27] Irradiation of WT 1c1c7 cells photosensitized with WST11 induced both an autophagic and apoptotic response in wild-type 1c1c7 cultures. These effects are similar to those obtained with NPe6.[10] Hence, the initial formation of different ROS upon irradiation of 1c1c7 cultures sensitized with WST11 vs. NPe6 was not a factor in photokilling or the induction of autophagy. The nature of the 'trigger' for autophagy after PDT remains unknown. A variety of ROS are formed and can influence the outcome.[26,27] Attempts to quantify the contributions of singlet oxygen, vs. other ROS products, to phototoxicity have been equivocal. However, scavenging studies suggest that $^{\bullet}O_2^-$ and H_2O_2 play a role in the phototoxicity of PDT.[28] Furthermore, both $^{\bullet}O_2^-$ and H_2O_2 have been implicated in the initiation of autophagy.[29,30] Formation of superoxide can lead to downstream production of H_2O_2.[26,27] We conclude that the type of ROS initially formed during PDT is not a major factor in the initiation of autophagy.

PDT directed against lysosomes was recently reported to be more effective at photokilling than when mitochondria were the target.[31] The authors proposed that "other factors, such as different initial targets or different mechanisms of cell death, may also contribute to the observed differences in photodynamic efficiency." We propose that the photodynamic efficiency of lysosomal photosensitizers reflects their ability to disrupt the autophagic process. Although the induction of autophagy appears to occur with most classes of photosensitizers,[10] only lysosomal sensitizers cause permeabilization and alkylation or frank destruction of endosomes and lysosomes. Such conditions should prevent lysosome fusion with amphisomes/autophagosomes resulting in an accumulation of the latter and the development of 'autophagic stress.'[32] The latter condition may facilitate the induction of, or amplification of an apoptotic response. Indeed, we have documented both the accumulation of autophagosomes[10] and the suppression of autophagic flux (**Fig. 5H**) following lysosomal photodamage. In essence, lysosomal photodamage negates autophagic prosurvival functions and further burdens the cell through the development of autophagic stress.

An ATG7 deficiency promoted resistance to the phototoxicity of both NPe6 and WST11. Procaspase activation was suppressed and cell survival increased in ATG7-deficient 1c1c7 cultures across a broad range of light doses. Similar results have been observed by other investigators who have used different toxicants. The most relevant study is by Walls et al.[33] These authors found

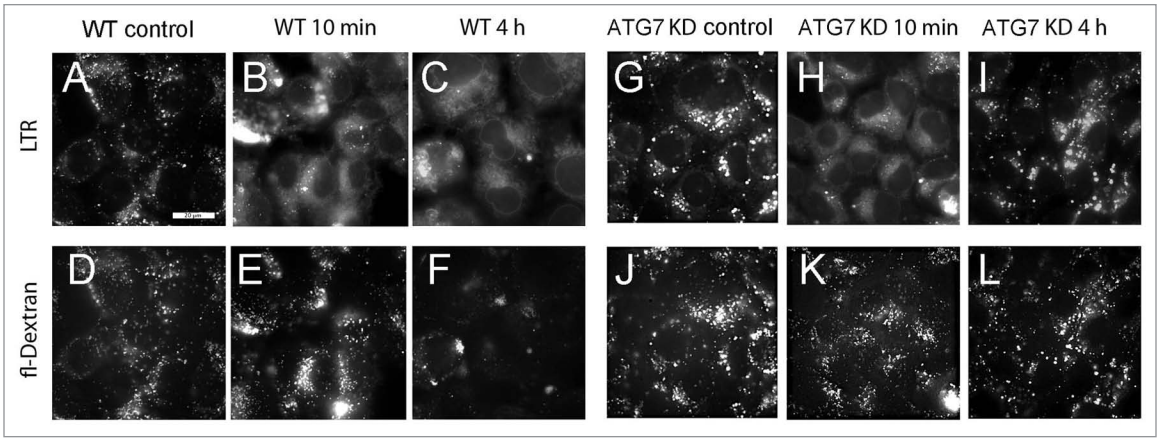

Figure 8. Analyses of lysosomal permeabilization following NPe6 PDT. Cultures of WT (A–F) and ATG7 KD (G–L) cells were preloaded with fluorescein-conjugated 10-kDa dextran polymers as described in Materials and Methods prior to being sensitized with 20 μM NPe6 and irradiated (270 mJ/cm^2). LTR was added to the cultures 10 min prior to imaging. LTR (A–C and G–I) and dextran (D–F and J–L) fluorescence were captured 10 min and 4 h after irradiation. Similar results were obtained in a second study.

that treatment of cultured neural precursor cells with chloroquine or bafilomycin A_1 caused autophagosome accumulation, suppressed autophagic flux, and ultimately induced apoptosis and cell death. An ATG7 knockdown suppressed the proapoptotic activities of chloroquine of bafilomycin A_1. In other studies it has been reported that ATG7 deficiency reduces sensitivity to the proapoptotic activities of etoposide,[34] staurosporine,[34] TGFB/TGF-β,[35] and 1,3-dibutyl-2-thiooxo-imidazolidine-4,5-dione (a generator of H_2O_2).[36] In each of these studies, proapoptotic concentrations of the different toxicants induced an autophagic response in wild-type cultures that preceded or paralleled the initiation of apoptosis. Although analyses of autophagic flux were not reported in these studies, it is worth noting that apoptotic concentrations of etoposide,[37,38] staurosporine[39] and H_2O_2,[38,40] induce endosomal/lysosomal permeabilization or rupture in a variety of cellular systems. In doing so, the effects of these agents on lysosomes may be analogous to lysosomal photosensitizers, and contribute to autophagosome accumulation and the development of autophagic stress.

A simple explanation for the observed survival of ATG7 KD cells in our PDT protocols is that autophagy is somehow involved in the induction of apoptosis by lysosomal photosensitizers. This seems unlikely for two reasons. First, apoptosis develops prior to autophagy in NPe6 sensitized WT 1c1c7 cultures irradiated with a very high light dose.[10] Second, although the capacity for developing an autophagic response was significantly suppressed in ATG5 KD cells, the latter were just as susceptible as WT 1c1c7 cells to the proapoptotic effects of NPe6 or WST11 PDT. If autophagy was necessary for the development of apoptosis following lysosomal photodamage, apoptosis should have been suppressed in ATG5 KD cells. This was not observed.

Photodamage catalyzed by NPe6 to WT 1c1c7 cultures under LD_{95} conditions resulted in the sequential loss of LTR and dextran-10,000 fluorescent puncta. Loss of dextran-10,000 fluorescent puncta is suggestive of frank lysosomal membrane permeabilization, a condition that would facilitate cathepsin leakage into the cytosol. We and others have shown that released lysosomal cathepsins are responsible for the initiation of NPe6 PDT-induced apoptosis,[19,41] and that treatments that inhibit their release suppress the process.[20,42] An ATG7 deficiency did not prevent initial photodamage to late endosomes/lysosomes, as monitored by the loss of the pH gradient needed for LTR accumulation (**Fig. 1F** and **Fig. 7B**). However, unlike WT or ATG5 KD 1c1c7 cultures, the lysosomes of ATG7 KD cells quickly recovered their ability to accumulate LTR within 4 h of irradiation. Furthermore, and more importantly, NPe6 PDT did not cause a frank permeabilization of lysosomal membranes in ATG7 deficient cells. Hence, it is conceivable that an ATG7 deficiency alters lysosomes such that they are less susceptible to oxidative damage, as occurs when lysosomes accumulate sphingomyelin[42] or non-esterified cholesterol.[20] Alternatively, an ATG7 deficiency may modulate ROS availability or upregulate a compensatory survival pathway. We are currently pursuing these issues.

In summary, lysosomal photodamage releases factors capable of activating the intrinsic apoptotic program, but also suppresses autophagic prosurvival functions and adds additional stress on the cells because of a block in the autophagic flux. The latter two effects may be unique to photosensitizers that target the lysosome, and may contribute to the overall efficacy of these agents. Moreover, ATG7 appears to play a role in facilitating lysosomal photodamage that is independent of its role in macroautophagy. As such, this appears to be a novel function for ATG7.

Materials and Methods

Chemicals and biological. WST 9 was provided by Steba Pharmaceuticals. WST11 was prepared from WST9 as described previously.[43] NPe6 was provided by Prof. Kevin M. Smith, Louisiana State University. MEM-Eagle α modification, (M0894) and HO33342 (B2261) were provided by Sigma-Aldrich. The fluorescent probes Lysotracker Red (L7528), HO33342 (H3570), MitoTracker Orange (M-7510), ER-Tracker (E-12353) and fluorescein-conjugated 10 kDa dextran polymers (D1820) were purchased from Invitrogen.

Cells and cell culture. Murine hepatoma 1c1c7 cells were grown on plastic culture dishes in a humidified atmosphere of air + 5% CO_2 in complete medium consisting of α-MEM supplemented with 5% fetal bovine serum (Atlanta Biologicals, S11150) and 100 units/mL penicillin + 100 μg/mL streptomycin (Invitrogen, 15140). The derivation of 1c1c7 cells that stably express shRNA to *Atg7* (i.e., 1c1c7 ATG7 KD) has been published.[11] 1c1c7 cells that stably express shRNA to murine *Atg5* (i.e., 1c1c7 ATG5 KD) were prepared by transfection with a mixture of 4 pRS plasmids that each express a different murine *Atg5* shRNA (OriGene, TR500113), followed by two weeks of selection in growth medium containing 1 μg/ml puromycin. The KD lines were periodically monitored by western blotting to insure continued significant silencing of *Atg5* or *Atg7*. The plating efficiencies and doubling times of the WT, ATG7 KD and ATG5 KD 1c1c7 cell lines were similar. 1c1c7 cells that stably express GFP-LC3 (i.e., 1c1c7 GFP-LC3) were generated by transfection of pEGFP-LC3m, which consists of a rat *Lc3* coding sequence cloned in a pEGFP-C1 vector (the gift of Drs. N. Mizushima and T. Yoshimori), followed by 2 wk of selection in complete medium + 400 μg/ml G418. At this point most resistant cells (> 95%) were positive for GFP fluorescence. After expansion, the transfected cells were aliquoted and stored at -80°C. The GFP-LC3 line is maintained in complete medium + 200 μg/ml G418, but transferred to G418-free medium prior to the initiation of any study. For studies involving microscopy, cells were cultured on 1 cm^2 glass coverslips placed at the bottom of plastic dishes.

PDT protocols. Cultures were incubated with 1 μM WST11 for 16 h, or with 20 μM NPe6 for 1 h. The medium was then replaced and the dishes irradiated with light provided by a 600-W quartz-halogen source filtered with 10 cm of water to remove infrared. For PDT studies involving WST11, the bandwidth was further confined to 750 ± 10 nm; for NPe6, 660 ± 10 nm, using interference filters (Oriel). Irradiation times were calculated based on clonogenic studies, so as to yield the desired effect on viability. For clonogenic studies approximately 250 cells were plated on 60 mm dishes, allowed to adhere for 24 h, then treated. Colonies of 30 or more cells were determined using an Oxford Optronix GelCount device. Three dishes were used per analysis.

Microscopy. All images involving phase and fluorescence microscopy were acquired with a Nikon E-600 microscope using a Rolera EM-C2 EMCCD camera (QImaging) and processed by MetaMorph software (Molecular Devices). For electron microscopy, cells were trypsinized and the cell pellets were fixed with glutaraldehyde and osmium tetraoxide, treated with uranyl acetate + lead citrate, and then dehydrated in ethanol. The resulting pellets were embedded in epon resin and cut with an ultramicrotome to a 70 nm thickness before viewing.

Phase-contrast images were assessed to evaluate vacuole formation and the appearance of apoptotic or necrotic morphology. Chromatin condensation was assessed by fluorescence using HO33342 as described previously,[6] using 330–380 nm excitation and measuring emission at 420–450 nm. HO33342 was added during the final 10 min of the incubation at 37° prior to viewing. The intracellular location of WST11 was assessed by monitoring its intrinsic fluorescence emission at wavelengths > 700 nm, using 330–380 nm excitation. GFP-LC3 fluorescence was monitored using 480 nm excitation and 505 nm emission. The procedure for the staining of acidic organelles (i.e., late endosomes and lysosomes) with LysoTracker Red involved a 10 min incubation at 37°C with a 100 nM concentration of the probe.[44] LTR fluorescence was monitored using 500–560 nm excitation and measuring emission at wavelengths > 590 nm. Labeling of mitochondria with Mitotracker Orange (MTO) and the endoplasmic reticulum with ER-Tracker involved a 10 min incubation of cultures with these probes (3 μM). The excitation/emission wavelength optima for MTO were 480/540 nm and for ER-Tracker, 370/440 nm.

For studies probing lysosomal integrity after photodamage, cultures were incubated with 30 μg/ml fluorescein-conjugated 10 kDa dextran polymers for 6 h. The medium was then replaced. After a 16 h chase NPe6 (20 μM) was added for an additional hour. The medium was then replaced and the cells irradiated using 270 mJ/cm^2. LTR was added for an additional 10 min and the fluorescence patterns of the two probes was determined. The procedure for LTR is described above. Dextran polymer fluorescence (510–600 nm) was measured using excitation centered at 470 nm.

DEVDase activation. Cleavage of a caspase-3/7 substrate containing the DEVD sequence and a quenched fluorophore (Molecular Probes/Invitrogen, E13184) was measured as described previously.[45] Cells were collected at specified intervals after irradiation for the assay, which was done in triplicate. A micro Lowry assay (Sigma-Aldrich, B3934, F9252) was used to estimate protein concentrations, using bovine serum albumin as the standard.

Western blotting. The conversion of LC3-I to LC3-II was monitored by western blotting as described previously.[10] To assess autophagic flux, some cultures were treated with 50 mM NH_4Cl for 2 h to block the processing of autophagosomes.[22]

Disclosure of Potential Conflicts of Interest

No potential conflicts of interest were disclosed.

Acknowledgments

This study was supported by grant CA 23378 from the National Cancer Institute. Ann Marie Santiago provided excellent technical assistance during the course of this work. We thank Dr. James Hatfield, Department of Pathology at the John Dingell VA Hospital, for acquisition of images involving electron microscopy. M. Price is a predoctoral trainee who was partially supported by National Cancer Institute grant T32 CA009531. We thank N. Mizushima and T. Yoshimori for providing the GFP-LC3 plasmid.

Supplemental Materials

Supplemental materials may be found here:
www.landesbioscience.com/journals/autophagy/article/20792

References

1. Dougherty TJ, Gomer CJ, Henderson BW, Jori G, Kessel D, Korbelik M, et al. Photodynamic therapy. J Natl Cancer Inst 1998; 90:889-905; PMID:9637138; http://dx.doi.org/10.1093/jnci/90.12.889
2. Agostinis P, Berg K, Cengel KA, Foster TH, Girotti AW, Gollnick SO, et al. Photodynamic therapy of cancer: an update. CA Cancer J Clin 2011; 61:250-81; PMID:21617154; http://dx.doi.org/10.3322/caac.20114
3. Agarwal ML, Clay ME, Harvey EJ, Evans HH, Antunez AR, Oleinick NL. Photodynamic therapy induces rapid cell death by apoptosis in L5178Y mouse lymphoma cells. Cancer Res 1991; 51:5993-6; PMID:1933862
4. Kim HR, Luo Y, Li G, Kessel D. Enhanced apoptotic response to photodynamic therapy after bcl-2 transfection. Cancer Res 1999; 59:3429-32; PMID:10416606
5. Xue LY, Chiu SM, Oleinick NL. Photochemical destruction of the Bcl-2 oncoprotein during photodynamic therapy with the phthalocyanine photosensitizer Pc 4. Oncogene 2001; 20:3420-7; PMID:11423992; http://dx.doi.org/10.1038/sj.onc.1204441
6. Kessel D, Castelli M. Evidence that bcl-2 is the target of three photosensitizers that induce a rapid apoptotic response. Photochem Photobiol 2001; 74:318-22; PMID:11547571; http://dx.doi.org/10.1562/0031-8655(2001)074<0318:ETBITT>2.0.CO;2
7. Chang NC, Nguyen M, Germain M, Shore GC. Antagonism of Beclin 1-dependent autophagy by BCL-2 at the endoplasmic reticulum requires NAF-1. EMBO J 2010; 29:606-18; PMID:20010695; http://dx.doi.org/10.1038/emboj.2009.369
8. Kessel D. Transport and localisation of m-THPC in vitro. Int J Clin Pract 1999; 53:263-7; PMID:10563069
9. Kessel D, Conley M, Vicente MG, Reiners JJ Jr. Studies on the subcellular localization of the porphycene CPO. Photochem Photobiol 2005; 81:569-72; PMID:15745423; http://dx.doi.org/10.1562/2004-12-16-RA-403.1
10. Reiners JJ Jr., Agostinis P, Berg K, Oleinick NL, Kessel D. Assessing autophagy in the context of photodynamic therapy. Autophagy 2010; 6:7-18; PMID:19855190; http://dx.doi.org/10.4161/auto.6.1.10220
11. Andrzejak M, Price M, Kessel DH. Apoptotic and autophagic responses to photodynamic therapy in 1c1c7 murine hepatoma cells. Autophagy 2011; 7:979-84; PMID:21555918; http://dx.doi.org/10.4161/auto.7.9.15865
12. Kessel D, Arroyo AS. Apoptotic and autophagic responses to Bcl-2 inhibition and photodamage. Photochem Photobiol Sci 2007; 6:1290-5; PMID:18046484; http://dx.doi.org/10.1039/b707953b
13. Xue LY, Chiu SM, Oleinick NL. Atg7 deficiency increases resistance of MCF-7 human breast cancer cells to photodynamic therapy. Autophagy 2010; 6:248-55; PMID:20083906; http://dx.doi.org/10.4161/auto.6.2.11077
14. Wang S, Bromley E, Xu L, Chen JC, Keltner L. Talaporfin sodium. Expert Opin Pharmacother 2010; 11:133-40; PMID:20001435; http://dx.doi.org/10.1517/14656560903463893
15. Spikes JD, Bommer JC. Photosensitizing properties of mono-L-aspartyl chlorin e6 (NPe6): a candidate sensitizer for the photodynamic therapy of tumors. J Photochem Photobiol B 1993; 17:135-43; PMID:8459317; http://dx.doi.org/10.1016/1011-1344(93)80006-U
16. Mazor O, Brandis A, Plaks V, Neumark E, Rosenbach-Belkin V, Salomon Y, et al. WST11, a novel water-soluble bacteriochlorophyll derivative; cellular uptake, pharmacokinetics, biodistribution and vascular-targeted photodynamic activity using melanoma tumors as a model. Photochem Photobiol 2005; 81:342-51; PMID:15623318; http://dx.doi.org/10.1562/2004-06-14-RA-199.1
17. Betrouni N, Lopes R, Puech P, Colin P, Mordon S. A model to estimate the outcome of prostate cancer photodynamic therapy with TOOKAD Soluble WST11. Phys Med Biol 2011; 56:4771-83; PMID:21753234; http://dx.doi.org/10.1088/0031-9155/56/15/009
18. Roberts WG, Liaw LH, Berns MW. In vitro photosensitization II. An electron microscopy study of cellular destruction with mono-L-aspartyl chlorin e6 and photofrin II. Lasers Surg Med 1989; 9:102-8; PMID:2523992; http://dx.doi.org/10.1002/lsm.1900090204
19. Reiners JJ Jr., Caruso JA, Mathieu P, Chelladurai B, Yin XM, Kessel D. Release of cytochrome c and activation of pro-caspase-9 following lysosomal photodamage involves Bid cleavage. Cell Death Differ 2002; 9:934-44; PMID:12181744; http://dx.doi.org/10.1038/sj.cdd.4401048
20. Reiners JJ Jr., Kleinman M, Kessel D, Mathieu PA, Caruso JA. Nonesterified cholesterol content of lysosomes modulates susceptibility to oxidant-induced permeabilization. Free Radic Biol Med 2011; 50:281-94; PMID:21074609; http://dx.doi.org/10.1016/j.freeradbiomed.2010.11.006
21. Caruso JA, Mathieu PA, Joiakim A, Leeson B, Kessel D, Sloane BF, et al. Differential susceptibilities of murine hepatoma 1c1c7 and Tao cells to the lysosomal photosensitizer NPe6: influence of aryl hydrocarbon receptor on lysosomal fragility and protease contents. Mol Pharmacol 2004; 65:1016-28; PMID:15044632; http://dx.doi.org/10.1124/mol.65.4.1016
22. Klionsky DJ, Abeliovich H, Agostinis P, Agrawal DK, Aliev G, Askew DS, et al. Guidelines for the use and interpretation of assays for monitoring autophagy in higher eukaryotes. Autophagy 2008; 4:151-75; PMID:18188003
23. Kessel D, Reiners JJ Jr. Apoptosis and autophagy after mitochondrial or endoplasmic reticulum photodamage. Photochem Photobiol 2007; 83:1024-8; PMID:17880495; http://dx.doi.org/10.1111/j.1751-1097.2007.00088.x
24. Ashur I, Goldschmidt R, Pinkas I, Salomon Y, Szewczyk G, Sarna T, et al. Photocatalytic generation of oxygen radicals by the water-soluble bacteriochlorophyll derivative WST11, noncovalently bound to serum albumin. J Phys Chem A 2009; 113:8027-37; PMID:19545111; http://dx.doi.org/10.1021/jp900580e
25. Kessel D, Price M. Evaluation of diethyl-3-3'-(9,10-anthracenediyl)bis acrylate as a probe for singlet oxygen formation during photodynamic therapy. Photochem Photobiol 2012; 88:717-20; PMID:22296586; http://dx.doi.org/10.1111/j.1751-1097.2012.01106.x
26. Henderson BW, Miller AC. Effects of scavengers of reactive oxygen and radical species on cell survival following photodynamic treatment in vitro: comparison to ionizing radiation. Radiat Res 1986; 108:196-205; PMID:3097749; http://dx.doi.org/10.2307/3576825
27. MacDonald IJ, Dougherty TJ. Basic principles of photodynamic therapy. J Porphyr Phthalocyanines 2001; 5:105-29; http://dx.doi.org/10.1002/jpp.328
28. Price M, Terlecky SR, Kessel D. A role for hydrogen peroxide in the pro-apoptotic effects of photodynamic therapy. Photochem Photobiol 2009; 85:1491-6; PMID:19659920; http://dx.doi.org/10.1111/j.1751-1097.2009.00589.x
29. Scherz-Shouval R, Shvets E, Fass E, Shorer H, Gil L, Elazar Z. Reactive oxygen species are essential for autophagy and specifically regulate the activity of Atg4. EMBO J 2007; 26:1749-60; PMID:17347651; http://dx.doi.org/10.1038/sj.emboj.7601623
30. Chen Y, Azad MB, Gibson SB. Superoxide is the major reactive oxygen species regulating autophagy. Cell Death Differ 2009; 16:1040-52; PMID:19407826; http://dx.doi.org/10.1038/cdd.2009.49
31. Rodriguez ME, Zhang P, Azizuddin K, Delos Santos GB, Chiu SM, Xue LY, et al. Structural factors and mechanisms underlying the improved photodynamic cell killing with silicon phthalocyanine photosensitizers directed to lysosomes versus mitochondria. Photochem Photobiol 2009; 85:1189-200; PMID:19508642; http://dx.doi.org/10.1111/j.1751-1097.2009.00558.x
32. Chu CT. Autophagic stress in neuronal injury and disease. J Neuropathol Exp Neurol 2006; 65:423-32; PMID:16772866; http://dx.doi.org/10.1097/01.jnen.0000229233.75253.be
33. Walls KC, Ghosh AP, Franklin AV, Klocke BJ, Ballestas M, Shacka JJ, et al. Lysosome dysfunction triggers Atg7-dependent neural apoptosis. J Biol Chem 2010; 285:10497-507; PMID:20123985; http://dx.doi.org/10.1074/jbc.M110.103747
34. Grishchuk Y, Ginet V, Truttmann AC, Clarke PG, Puyal J. Beclin 1-independent autophagy contributes to apoptosis in cortical neurons. Autophagy 2011; 7:1115-31; PMID:21646862; http://dx.doi.org/10.4161/auto.7.10.16608
35. Kiyono K, Suzuki HI, Matsuyama H, Morishita Y, Komuro A, Kano MR, et al. Autophagy is activated by TGF-β and potentiates TGF-β-mediated growth inhibition in human hepatocellular carcinoma cells. Cancer Res 2009; 69:8844-52; PMID:19903843; http://dx.doi.org/10.1158/0008-5472.CAN-08-4401
36. Wong CH, Iskandar KB, Yadav SK, Hirpara JL, Loh T, Pervaiz S. Simultaneous induction of non-canonical autophagy and apoptosis in cancer cells by ROS-dependent ERK and JNK activation. PLoS One 2010; 5:e9996; PMID:20368806; http://dx.doi.org/10.1371/journal.pone.0009996
37. Emert-Sedlak L, Shangary S, Rabinovitz A, Miranda MB, Delach SM, Johnson DE. Involvement of cathepsin D in chemotherapy-induced cytochrome c release, caspase activation, and cell death. Mol Cancer Ther 2005; 4:733-42; PMID:15897237; http://dx.doi.org/10.1158/1535-7163.MCT-04-0301
38. Nylandsted J, Gyrd-Hansen M, Danielewicz A, Fehrenbacher N, Lademann U, Høyer-Hansen M, et al. Heat shock protein 70 promotes cell survival by inhibiting lysosomal membrane permeabilization. J Exp Med 2004; 200:425-35; PMID:15314073; http://dx.doi.org/10.1084/jem.20040531
39. Kågedal K, Johansson AC, Johansson U, Heimlich G, Roberg K, Wang NS, et al. Lysosomal membrane permeabilization during apoptosis--involvement of Bax? Int J Exp Pathol 2005; 86:309-21; PMID:16191103; http://dx.doi.org/10.1111/j.0959-9673.2005.00442.x
40. Kurz T, Gustafsson B, Brunk UT. Intralysosomal iron chelation protects against oxidative stress-induced cellular damage. FEBS J 2006; 273:3106-17; PMID:16762036; http://dx.doi.org/10.1111/j.1742-4658.2006.05321.x
41. Wan Q, Liu L, Xing D, Chen Q. Bid is required in NPe6-PDT-induced apoptosis. Photochem Photobiol 2008; 84:250-7; PMID:18173728; http://dx.doi.org/10.1111/j.1751-1097.2007.00248.x
42. Caruso JA, Mathieu PA, Reiners JJ Jr. Sphingomyelins suppress the targeted disruption of lysosomes/endosomes by the photosensitizer NPe6 during photodynamic therapy. Biochem J 2005; 392:325-34; PMID:15943580; http://dx.doi.org/10.1042/BJ20050313
43. Brandis A, Mazor O, Neumark E, Rosenbach-Belkin V, Salomon Y, Scherz A. Novel water-soluble bacteriochlorophyll derivatives for vascular-targeted photodynamic therapy: synthesis, solubility, phototoxicity and the effect of serum proteins. Photochem Photobiol 2005; 81:983-93; PMID:15839743; http://dx.doi.org/10.1562/2004-12-01-RA-389R1.1
44. Kessel D, Oleinick NL. Initiation of autophagy by photodynamic therapy. Methods Enzymol 2009; 453:1-16; PMID:19216899; http://dx.doi.org/10.1016/S0076-6879(08)04001-9
45. Kessel D, Reiners JJ Jr., Hazeldine ST, Polin L, Horwitz JP. The role of autophagy in the death of L1210 leukemia cells initiated by the new antitumor agents, XK469 and SH80. Mol Cancer Ther 2007; 6:370-9; PMID:17237296; http://dx.doi.org/10.1158/1535-7163.MCT-05-0386